Hindawi
International Journal of Polymer Science
Volume 2018, Article ID 8527693, 10 pages
https://doi.org/10.1155/2018/8527693

Research Article

Preparation of Miscible PVA/PEG Blends and Effect of Graphene Concentration on Thermal, Crystallization, Morphological, and Mechanical Properties of PVA/PEG (10wt%) Blend

Fahad H. Falqi,[1] Osamah A. Bin-Dahman,[2] M. Hussain,[3] and Mamdouh A. Al-Harthi[1]

[1]*Department of Chemical Engineering, King Fahd University of Petroleum and Minerals, Dhahran 31261, Saudi Arabia*
[2]*Department of Chemical Engineering, Faculty of Engineering and Petroleum, Hadhramout University, Mukalla, Yemen*
[3]*Department of Materials and Chemical Engineering, Hanyang University, Seoul, Republic of Korea*

Correspondence should be addressed to Mamdouh A. Al-Harthi; mamdouh@kfupm.edu.sa

Received 15 April 2018; Revised 19 July 2018; Accepted 9 August 2018; Published 12 September 2018

Academic Editor: Yulin Deng

Water-soluble polymers such as poly(vinyl alcohol) (PVA) and poly(ethylene glycol) (PEG) and their nanocomposites with graphene were prepared by using a solution mixing and casting technique. The effect of different PEG loadings was investigated to determine the optimum blend ratio. The films were characterized using Fourier transform infrared spectroscopy (FTIR), differential scanning calorimetry (DSC), and thermogravimetric analyzer (TGA) methods. Also, the mechanical properties including tensile strength and elongation at break were measured using a universal tensile testing machine. FTIR results confirmed the formation of the H-bond between PEG and PVA. DSC studies revealed that PEG has a significant plasticization effect on PVA as seen by the drop in the glass transition temperature (T_g). The blend with 10 wt% PEG loading was found to be the optimum blend because of good compatibility as shown by FTIR and SEM results and improved thermal properties. PVA/PEG (10%) nanocomposites were prepared using graphene as a nanofiller. It was found that the elongation at break increased by 62% from 147% for the PVA/PEG (10%) blend to 209% for the nanocomposite with graphene loading of 0.2 wt%. The experimental values of tensile strength were compared using the predictive model of Nicolais and Narkis.

1. Introduction

Usage of polymeric thermoplastics has increased remarkably over the past four decades. Applications include grocery, merchandise, trash bags, food containers, caps and closures, plastic fuel tanks, drink cups, home appliances, cooking utensils, children's toys, and construction materials, among others. Water-soluble polymers such as PEG and PVA and their blends have found many applications such as packaging [1], cosmetics [2], and emulsifiers and adhesives [3], among others. PVA and its composites have been extensively studied by our group [1, 4–15]. With some modifications of the existing polymers, products with low cost and light weight may be developed for a wide range of applications with desirable properties such as mechanical, thermal, and optical properties. This makes them suitable as replacements for other traditional engineering materials such as metals. In recent years, biodegradable polymeric materials have been found useful for drug delivery, pharmaceuticals, paints, textiles, and tissue engineering applications [7, 16]. They have many uses, with many new applications involving blends of these polymers with other polymers and other materials [17]. Different physical and chemical treatment methods are available to modify these materials and make them successful in different fields. Blending is a simple and effective method to develop new materials with tailored properties. Recently, nanocomposites with improved properties have been prepared by mixing different polymers through the physical blending method. This is now a promising trend in the science of nanocomposites [18]. Studies on PVA/PEG blends

have been an active area for research that has attracted great commercial interest.

Studies have considered the potential to obtain materials with improved properties for various applications. Abdel Tawab et al. [19] studied the influence of the PEG content on PVA and found that the PEG content up to 60% can provide the best compatibility of the PVA/PEG blend. Other authors report PVA/PEG blends with a good film and reported that blends with PEG content above 40% do not form a cast film due to phase separation [19]. However, the main disadvantage of hydrophilic polymers such as PVA and PEG studied here is their weak mechanical properties [20]. The nanomaterials at very low loading content revealed improved properties for nanocomposite systems when incorporated into the polymer matrix [8, 21]. Nanofillers, especially carbon nanomaterials, have led to remarkably improved properties, at very low loading content, when incorporated into the polymer matrix. In particular, polymer composites of carbon nanotubes (CNT) and graphene have attracted a wide range of applications in modern science and technology. These fillers can provide unique properties to the polymer matrices [22]. Graphene has been given special attention due to its unique properties [23]. It is fabricated from natural graphite and is cheaper compared to other fillers such as CNT [24].

PVA can be effectively reinforced by using graphene nanosheets [1]. El Sayed and Morsi [25] prepared PVA/PEG nanocomposites based on a hematite (α-Fe_2O_3) nanofiller and reported improvement in optical and dielectric properties of the prepared nanocomposites. They found that both the refractive index and ac conductivity increased significantly as a function of increasing the filler content [25]. It was also reported that addition of α-Fe_2O_3 nanoparticles improved the thermal stability of PVA [22]. Sengwa et al. [18] used nanoclay and studied the effect of its addition on PVA/polyethylene oxide (PEO) blend. PVA/PEG nanocomposites have also been prepared and studied using montmorillonite (MMT) clay as nanofiller [20]. The hydrophilic characteristic of MMT clay helps their dispersion into water-soluble polymers such as PVA and PEG [20]. The addition of MMT up to 4 wt% improves the mechanical properties of the PVA matrix [26].

To the best of our knowledge and survey of literature, the study of the PVA/PEG nanocomposite based on graphene has not been previously reported. Therefore, in this work, the effect of PEG loadings on PVA/PEG blends is first studied in an attempt to obtain cast films with good physical properties to be used for further investigation. Also, PVA/PEG nanocomposites were prepared using graphene as a nanofiller to investigate its influence on the mechanical properties of the PVA/PEG blend.

2. Experimental

2.1. Materials. Polyethylene glycol (PEG) (powder, molecular *weight* = 4000 *g*/*mol*) and polyvinyl alcohol (PVA) (degree of *hydrolysis* = 99%, molecular *weight* = 27,000 *g*/*mol*) were supplied by Sigma-Aldrich Company, USA. Both homopolymers were used for the preparation of PVA/PEG blends and PVA/PEG nanocomposites as received from the supplier without further purification. Graphene, trade name GRAFEN®-iGP, of a purity of 96–99% and thickness of 50–100 nanometers, was procured from Grafen Chemical Industries, Turkey.

2.2. Preparation of PVA/PEG Blends. The films for pure PVA and PEG/PVA blends were prepared using the solution cast method. After many experimental trials, acceptable films with good transparency were only obtained for pure PVA and PVA/PEG blends with PEG loadings at 5, 10, 15, and 20 wt%, while loss of transparency and occurrence of phase separation were observed for the prepared blends containing PEG above this loading range. Films possessing acceptable transparency (as seen by visual observation) were obtained for the blends shown in Table 1, which have PEG loading (<20 wt%). The obtained films of these blends along with that of pure PVA were characterized and investigated. However, for other blends prepared as part of this experimental work, PEG loadings included 30, 40, 50, 60, and 70 wt%. These films were very brittle due to the higher PEG content which caused a phase separation between the two blended polymers, PVA and PEG. For this reason, these polymer blends were not considered to be suitable for characterization and were discarded.

For the preparation of PEG/PVA blends, different weighted amounts of PEG and PVA were separately dissolved in deionized water based on the formulations shown in Table 1. A fixed amount of PVA (3 g) was used in all PVA/PEG blends. PVA was used in the blends since PVA gives good film with improved flexibility and mechanical stability [20]. Mixtures of the polymers were stirred at 400 rpm and 80°C for 2 hr to ensure complete dissolution/mixing. Then, the whole mixture was degassed in a vacuum oven for 10 min. The solution was then poured into a petri dish and left to dry at room temperature for 6 days. Finally, the obtained film was peeled off from the petri dish and preserved in a desiccator filled with silica gel to avoid moisture uptake [1]. The obtained films for all samples were kept and used for further characterization.

2.3. Preparation of PVA/PEG Nanocomposites. The same procedure mentioned above for the preparation of the films of PVA/PEG blends was followed for the preparation of PVA/PEG nanocomposite films. PVA/PEG nanocomposites were prepared based on the optimum blend ratio of PVA/PEG found in the previous step and using graphene as a nanofiller. Graphene at different loadings (0.1, 0.2, 0.3, 0.5, and 1 wt%) was separately mixed with water, and the aqueous suspension was sonicated for 2 min. Then, the solution was mixed with that of the PVA/PEG blend and stirred for 2 h at 80°C followed by a degassing step and casting similar to the above procedure. The obtained films of PVA/PEG nanocomposites were kept in the same desiccator utilized for PVA/PEG blends and used for further characterization.

2.4. Characterization

2.4.1. Thermal Properties. Differential scanning calorimetry (DSC) and thermogravimetric (TG) studies of the obtained

Table 1: The formulations for the prepared PVA/PEG blends.

Sample code	PEG content (wt%)	PVA content (wt%)
Pure PVA	0	100
PVA/PEG (5%)	5	95
PVA/PEG (10%)	10	90
PVA/PEG (15%)	15	85
PVA/PEG (20%)	20	80

films for pure PVA and PVA/PEG blends were carried out to evaluate their thermal and degradation behavior. The thermal properties such as heat of fusion or melting enthalpy (ΔH_{fus} or ΔH_m), melting temperature (T_m), crystallization temperature (T_c), and glass transition temperature (T_g) of all obtained films were evaluated by the DSC method. The DSC thermograms were obtained using DSC-Q1000, Universal V4.2E from TA Instruments. The DSC procedure followed three steps: heating/cooling/heating. In the first step, the films were heated from a temperature of −100 to 250°C at a heating rate of 10°C/min and held at this temperature for 5 min to eliminate the effects from the thermal history. Then, cooling was performed at a cooling rate of 10°C/min followed by a final heating step at the same heating rate of 10°C/min. The DSC experiments were carried out under nitrogen atmosphere with the flow rate of nitrogen gas set at 50 mL/min. Integration of the DSC thermograms over the plot range of 190–240°C allows determination of the heats of fusion [2, 16]. The degree of crystallinity (X_c) was calculated using the values of the measured heats of fusion according to (1) [27]:

$$X_c(\%) = \frac{\Delta H_{fus}/\varnothing_{PVA}}{\Delta H^o_{fus}} \times 100, \quad (1)$$

where ΔH_{fus} is the heat of fusion of PVA measured from DSC thermograms, $\varnothing_{PVA}$ is the PVA fraction in the composites, and ΔH^o_{fus} is the melting enthalpy of the totally crystallized PVA that is assumed to be 142 J/g [28].

The thermal behavior and stability were also evaluated for all obtained films using a thermogravimetric analyzer (TGA, Perkin Elmer Pyris 6). All samples were heated from 35 up to 600°C at a heating rate of 10°C/min. From the obtained TGA curves, the weight loss at different temperatures and the thermal degradation temperatures were measured for all samples. The differential thermogravimetric (DTG) thermograms were also developed by taking the first-order derivative of the corresponding TGA curves.

2.4.2. Fourier Transform Infrared (FTIR) Spectroscopy. FTIR (Nicolet 6700 Spectrometer) was used for obtaining the absorption spectra for the obtained films. All spectra were obtained by averaging 32 scans at a resolution of 4 cm^{-1} and recorded in the wave numbers ranging from 4000 to 500 cm^{-1}.

2.4.3. Mechanical Properties. The mechanical properties such as tensile strength and percentage of elongation at break were measured for the obtained films using a Universal Testing Instrument (Instron 3366). The films were cut (dog-bone shape with a gauge length of 25 mm) and tested at a constant cross-head speed of 10 mm/min at room temperature of 25°C. The recorded value for the measured parameters obtained from the stress-strain curves was taken as the average of at least three measurements to obtain reliable data.

The experimental data of the tensile strength were analyzed by comparing to some predicted models to understand the formation of weak structure in the composite [29, 30]. The tensile strength of the composites was predicted using the following empirical equation developed by Nicolais and Narkis [31] as described in (2).

$$\sigma_c = \sigma_m\left(1 - V_f^{2/3}\right), \quad (2)$$

where σ_c is the TS of the composite, σ_m is the TS of the polymer matrix, and V_f is the volume fraction of the filler. The mass fraction of graphene was converted to volume fraction using the value of graphene density 1.18 g/m^3. The assumptions made for this model include the following: (1) there is no adhesion between the filler particle and polymer matrix with a coefficient value of 1.21 for $V_f^{2/3}$, and (2) the particles are spherical.

2.4.4. Morphological Analysis. The morphology of the fracture surfaces of the films was examined by using a scanning electron microscope (LAYRA3 TESCAN FE-SEM). The samples were cryofractured by immersing the films in liquid nitrogen for 2 min and coated with a thin layer of gold to render the surface conductive prior to taking scanning electron micrograph images at an accelerating voltage of 5 kV.

3. Results and Discussion

3.1. Effect of PEG Loadings on PVA/PEG Blends. While PEG is hydrophilic and gives a clear solution, it is known to be difficult to achieve a good cast film using PEG [19]. On the other hand, PVA is known to form a good film when it is blended with other polymers [7, 8, 10]. It was noticed that at higher PEG loadings (above 20 wt%), it was difficult to get acceptable films that can be utilized for characterization. While blending PEG with PVA in the presence of water using a solution casting technique forms an H-bonded network to achieve miscibility, it was found difficult to obtain cast films due to phase separation [18, 32]. Abd Alla et al. [32] report that the PVA/PEG blend has shown limited compatibility in the range of 0–30 wt% of PEG. It was also reported that PVA/PEG blends containing 60, 70, and 80% PVA form acceptable cast films with acceptable physical properties [19].

The miscibility is an important factor in the study of polymer blends as the final properties of the blends are directly related to the degree of their miscibilities [2]. Generally, miscible polymer blends show one phase while immiscible blends show separated domains. Also, miscible polymeric blends show a decrease in the Gibbs energy of mixing [33]. Phase separation was observed for PVA/PEG blends with PEG content higher than 40%, while good films were obtained at lower PEG content. Transparent films were obtained for PVA/PEG blends containing PEG up to 30%,

which was attributed to the miscibility of both PEG and PVA homopolymers. However, the miscibility decreased with increasing PEG content above that limit. At higher PEG loading (above 30%), incompatibility was observed in PVA/PEG blends [32]. A similar finding was reported for poly(lactic acid) (PLA)/PEG blend which showed brittle nature at higher PEG content due to the lack of adhesion between the separate phase [34]. In another study, a phase separation was found in the PVA/starch blend at higher glycerol loading (glycerol was used as a plasticizer) which caused inhomogeneity and crystallinity drop [4]. This phenomenon was also observed in this work for the blends with PEG loading above 20 wt%, as explained earlier.

3.1.1. FTIR Analysis. FTIR spectroscopy is one of the most common techniques which provides useful information regarding the interactions between their functional groups. It is also considered a powerful method for studying the conformational changes in biopolymer systems [35]. The FTIR spectra of pure PVA and its blends at various PEG loadings in the wave number range of 4000–500 cm^{-1} are shown in Figure 1(a). Both polymers have good solubility in water. This is because of the formation of strong H-bonds between the functional group of the polymers and water molecules (hydrophilic property). It is clear from the spectra of all PVA/PEG blends that extensive H-bonding exists in the range 3000–3500 cm^{-1} due to stretching vibration of –OH groups which results from strong H-bonds that form during blending. For pure PVA, the spectra show a broad band centered at 3300 cm^{-1} associated with the stretching vibration of hydroxyl groups (–OH) present in the PVA structure. Similar results are reported by others [2, 32, 36]. Moreover, the FTIR spectra for all blends displayed almost similar absorption bands as pure PVA in the entire wavelength range, which indicates that the main functional groups in PEG and PVA are preserved [37]. However, there was a slight shift observed for peak position and relative intensity of the stretching vibration of the hydroxyl group (–OH) for all blends, which is attributed to the H-bonding formation between PVA and PEG at different PEG contents [38].

The characteristic absorption peaks of PVA/PEG blends that were observed at wavelengths 1330, 1421, 1100, 3300, and 851 cm^{-1} correspond respectively to C–O–C, C_6H_6, C–C, –OH, and C–H [39]. A strong absorption peak was also observed at 2900 cm^{-1} and linked to the stretching mode of the CH_2 group [36]. The absorption band at 1650 cm^{-1} was due to C=O stretching of the ester group formed in the PVA polymer during its preparation process. At higher PEG loadings above 10%, this peak disappeared due to the presence of a high amount of PEG. The stretching vibrations of C–C and C–O–C were observed at 1100 and 1330 cm^{-1} in the spectra, and their intensity values were changed at different PEG loadings. From Figure 1(b), the absorption band of –OH groups observed in the range 3000–3500 cm^{-1} got wider and with higher intensity in the spectra of the nanocomposites indicating occurrence of H-bond interactions between the –OH groups present in the blend and the oxygen groups of graphene [1, 9, 23]. However, there is a decrease in the intensity of the –OH band in the spectra of the nanocomposites with higher content of graphene. This may be attributed to the agglomeration of graphene sheets which causes a weakness in H-bond interactions.

3.1.2. Differential Scanning Calorimetry (DSC) Analysis. DSC is a very useful technique used to investigate the thermal properties of polymeric materials. The DSC thermograms obtained for PVA and its blends at different PEG loadings are shown in Figures 2(a) and 2(b). The thermal properties obtained from these thermograms are summarized in Table 2. PEG loading clearly has influence on the thermal properties of PVA/PEG blends.

Upon addition of PEG to the blends, the melting temperatures for all PVA/PEG blends were not much changed as compared to that of pure PVA, indicating that the T_m of PVA was not affected by PEG. From the heating curves shown in Figure 2(a), the measured melting enthalpy of the pure PVA film was 51.35 J/g. Blending PEG with PVA affected the crystallization behavior of PVA, and the crystallinity changed at different PEG loadings. A drop in crystallinity was observed for almost all blends containing PEG. The decrease in the crystallinity was attributed to the reduction of PVA chain mobility and the formation of H-bonding between PEG and PVA during the blending process, which hindered the crystallization step. Similar findings are reported, where a decrease in crystallinity was found for PVA/PEG blends when PEG of 10 wt% was used in the blends [2].

The endothermic peaks observed in the low-temperature region in the DSC heating curves of all PVA/PEG blends shown in Figure 2(a) were possibly associated with the T_g of the blends [40]. In another study, the melting of PEG was assumed to be responsible for these peaks [37]. As can be seen from Table 2, T_g decreased when adding PEG into PEG/PVA blends. Similar results were reported by others indicating the plasticization effect of PEG on PVA [41]. Li et al. [3] reported that effective plasticization for PVA was observed with PEG content <20 wt% as indicated by DSC results. Little difference in T_g values was observed for PVA/PEG blends at all of the different PEG loadings [3]. The cooling curves shown in Figure 2(b) for the PVA/PEG blend with 5 and 10 wt% PEG show two main crystallization events related to the crystallization temperatures of PEG and PVA. Since the difference between the two temperature values is high, it is reported that the crystallization of PEG had no effect on the crystallization behavior of PVA [3]. It was also noticed that the blends containing 15 and 20 wt% of PEG showed another smaller peak at around 25°C which could be due to the presence of incompatibility in these blends containing high PEG content [32].

3.1.3. Thermogravimetric Analysis (TGA). The integral (TGA) and derivative (DTG) thermograms can provide useful information regarding the thermal stability and the degradation behavior of the polymeric materials [24]. The TGA and DTG thermograms of the obtained films of the pure PVA and PVA/PEG blends at different PEG loadings are shown in Figure 3. The figure clearly shows the dependency of the thermal behavior on PEG loading. It was observed that

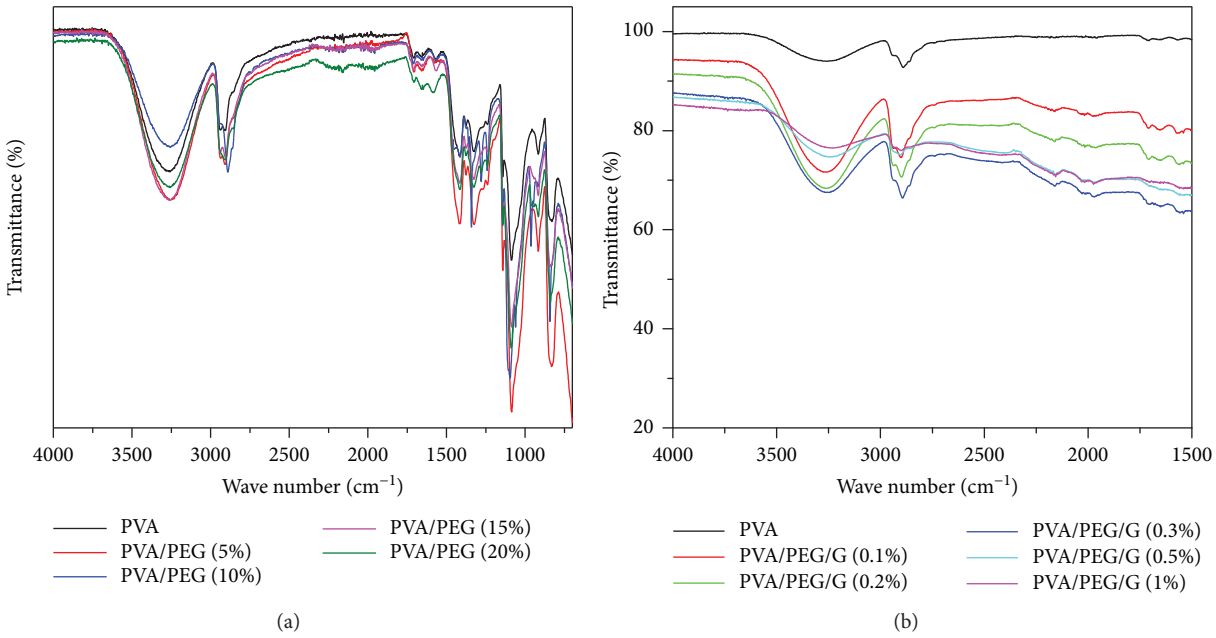

Figure 1: FTIR spectra for (a) PVA and its blends at different PEG loadings and (b) PVA/PEG nanocomposites at different graphene loadings.

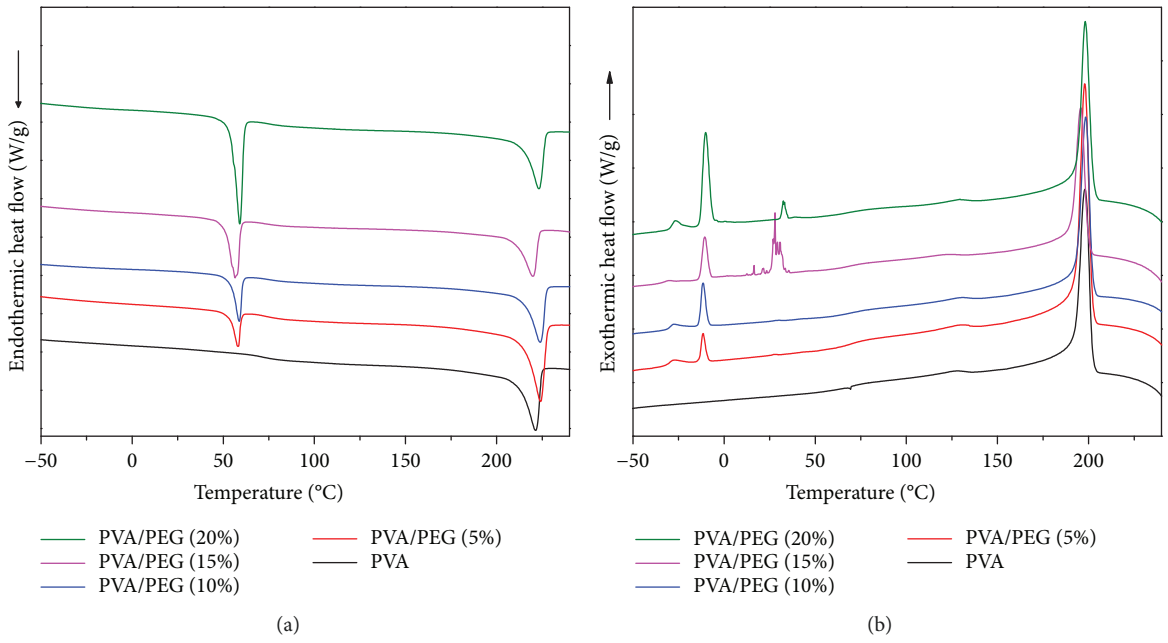

Figure 2: DSC thermograms for PVA and its blends at different PEG loadings: (a) heating curves and (b) cooling curves.

most of the blends showed better thermal stability compared to the pure PVA resulting from the shift of the degradation temperatures to higher values as shown in Figure 3.

Various steps can be seen in the TGA curves shown in Figure 3(a) for PVA/PEG blends; for example, the first process occurred up to around 90°C. The first one was related to the loss of physisorbed water [38, 42]. The major degradation of pure PVA was observed in a temperature range of 243–387°C [6]. PEG has higher thermal stability than PVA, and its thermal decomposition begins above 330°C [37, 38]. The products resulting from the thermal degradation of PEG were reported to include aldehydes, ketones, and ethers. On the other hand, the thermal decomposition products from PVA have been found to be water, aldehydes, and ketones up to a temperature of 240°C and above 240°C were alkanes, alkenes, and aromatic or unsaturated hydrocarbons [43, 44].

From the DTG curves shown in Figure 3(b), the maximum weight loss rates and the percent of residue at 550°C for all samples were obtained and are provided in Table 3.

Table 2: DSC data for PVA and PVA/PEG blends.

Sample code	T_m (°C)[a]	ΔH_m (J/g)[b]	T_c (°C)[c]	ΔH_c (J/g)[d]	T_g (°C)[e]	X_c (%)[f]
Pure PVA	211.78	51.35	198.12	84.74	83	36.16
PVA/PEG (5%)	214.43	55.21	197.81	80.88	53.85	38.88
PVA/PEG (10%)	214.79	45.29	198.52	73.94	54.39	31.89
PVA/PEG (15%)	210.15	31.98	195.67	63.16	51.34	22.52
PVA/PEG (20%)	214.21	42.23	198.07	68.22	54.47	29.74

[a]Melting temperature. [b]Melting enthalpy. [c]Crystallization temperature. [d]Enthalpy of crystallization.[e]Glass transition temperature. [f]Degree of crystallinity calculated by using (1).

For pure PVA, two peaks were observed at 280 and 440°C, which is in agreement with other findings [3]. A gradual increase in the peak width was observed with the increase in PEG content which is attributed to the changes in the heterogeneity of the blend composition [5]. It was observed that the weight loss rate decreased with the increase in PEG loading with a maximum value of about 1.7 wt%/°C (reached for the PVA/PEG blend with 5% PEG content). The addition of PEG to the blends formed H-bonds with PVA segments causing the decrease in the weight loss rate [5]. It was also noticed that the blend with 10% PEG showed the lowest residue value compared to other blends. While the other two blends loaded with PEG of 15 and 20% show lower loss rate values, their obtained films tend to be brittle due to phase separation and less compatibility resulting in weak mechanical properties as discussed below.

3.1.4. Mechanical Analysis. Since the blending process is expected to have an influence on the mechanical properties of the blends, a mechanical test was carried out for the pure PVA and its blends. However, it was not possible to perform the mechanical test for the obtained film of the blend containing 20 wt% PEG due to its high brittleness which prevented obtaining the required dog-bone shape of film for testing. However, the obtained films for the pure PVA and remaining blends at PEG loadings of 5, 10, and 15 wt% were successfully tested, and their mechanical properties including the tensile strength and the elongation at break were obtained from their corresponding tensile stress-strain curves as provided in Table 4.

The addition of PEG caused a drop in the tensile strength as compared to that for pure PVA due to the brittle PEG component. This is in agreement with other reported findings [19, 32]. This drop can also be attributed to the plasticizing effect of PEG with the pure PVA matrix [43]. Also, the tensile strength of PVA/PEG blends decreased with the increase in PEG loading. On the contrary, the elongation at break increased with the addition of PEG up to 10 wt% (PEG was used as a plasticizer to PVA). When PEG with moderate molecular weight (MW = 2000 and 4000) was used as a plasticizer for PLA/starch blend, the elongation at break was increased for the blend [45].

PVA/PEG blends with 5 and 10 wt% PEG loadings showed better tensile strength and elongation-at-break values compared to that at 15 wt% PEG loading, which can be attributed to the improvement of miscibility [19]. These improved mechanical properties can make the PVA/PEG blend a suitable candidate for industrial applications requiring better bending and strength features [39]. For the blend with 15 wt% PEG, the obtained film was observed to be brittle and showed phase separation due to the high content of PEG. This resulted in a significant drop in its measured mechanical properties including tensile strength and elongation at break.

3.2. Effect of Graphene Loadings on PVA/PEG Nanocomposites. Based on the results obtained and discussed for PVA/PEG blends, it can be concluded that the PEG loading at 10 wt% gives the optimum PVA/PEG blend and this was used for preparation of nanocomposites based on graphene for further studies. For simplicity, the optimum blend and graphene are abbreviated in the next sections as PVA/PEG and G, respectively.

3.2.1. Mechanical Properties. The mechanical properties of the blend and its nanocomposites at different graphene loadings were obtained from the mechanical test curves and are provided in Table 5. It is expected that some of the mechanical properties of the polymer blend can be improved by the addition of graphene as a nanofiller owning to the dispersion of the graphene nanoparticles having a large interfacial area and high aspect ratio into the polymer matrix. The homogenous dispersion of graphene in the polymer matrix is considered a crucial factor to improving the mechanical properties of graphene-based polymer nanocomposites [23]. Table 5 shows the influence of graphene on the mechanical properties of the PVA/PEG blend. Incorporation of graphene especially at low loading levels caused a fall in the tensile strength of the PVA/PEG nanocomposites. It is believed that the graphene nanosheets disperse individually at low graphene loading [1]. Also, it was observed that no significant difference in tensile properties of the PVA/PEG nanocomposites loaded with graphene up to 0.5 wt%. On the contrary, the elongation at break for the PEG/PVA nanocomposites was significantly increased as compared to that of the unfilled polymer blend. For example, the elongation at break increased by 62% from 147% for the blend to 209% for the nanocomposite with graphene loading of 0.2 wt%. Similar findings were reported, where the elongation at break increased by 70% when 0.7 wt% of reduced graphene oxide (RGO) was added to the PVA matrix [46]. However, with further addition of graphene above 0.3 wt%, the elongation at break gradually decreased which could be attributed to the increase in the brittleness of the obtained nanocomposite films at higher content of graphene.

Table 5 shows also the predicated tensile strength for PVA/PEG nanocomposites at different graphene loadings calculated by (2). A good agreement between the experimental and the predicated data was observed up to a graphene loading of 0.5 wt%. However, the increase in graphene loading above this limit caused a deviation between predicated tensile strength and its corresponding experimental data. This indicates the presence of weak interactions between the blend and graphene [47] as reported earlier in FTIR results.

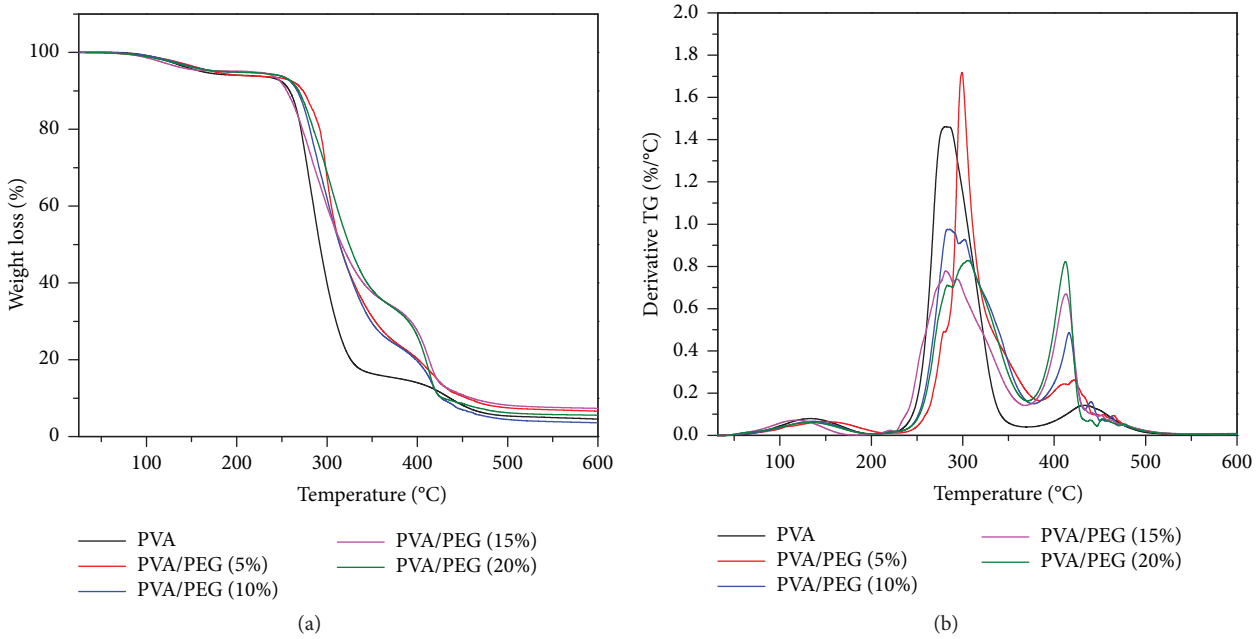

Figure 3: Thermograms for PVA and its blends at different PEG loadings: (a) TGA and (b) DTG.

Table 3: The maximum weight loss rates of PVA and its blends at different PEG loadings.

Sample code	Maximum weight loss rate (wt%/°C)	Residue at 550°C (%)
Pure PVA	1.46	5
PVA/PEG (5%)	1.7	6.96
PVA/PEG (10%)	0.98	3.88
PVA/PEG (15%)	0.76	7.6
PVA/PEG (20%)	0.82	5.7

Table 4: Mechanical properties of PVA and the blends at different PEG loadings.

Sample code	Tensile strength (MPa)	Elongation at break (%)
Pure PVA	45.86	101.99
PVA/PEG (5%)	33.24	172.73
PVA/PEG (10%)	30.67	147.34
PVA/PEG (15%)	27.88	27.89
PVA/PEG (20%)	nd	nd

Note: nd: not determined.

3.2.2. Scanning Electron Microscopic (SEM) Studies. The SEM image of the PVA/PEG blend containing no graphene presented in Figure 4(a) shows a homogeneous phase with no occurrence of phase separation indicating the excellent miscibility of PVA and PEG at this blend ratio. There is definite change in surface morphology with the incorporation of graphene into the blend as shown in Figures 4(b) and 4(f), resulting in an increase in the elongation at break for the nanocomposites with graphene loading up to 0.2% compared to the PVA/PEG blend reported previously in mechanical property studies [1]. The obtained films were seen not brittle and can be easily folded indicating higher flexibility and hence higher elongation at break [48]. However, at higher graphene loading, the elongation at break was decreased due to the agglomeration of graphene sheets which was clearly observed at a graphene loading of 1% as shown in Figure 4(f).

Table 5: Mechanical properties of PVA/PEG blend and its nanocomposites at different graphene loadings.

Sample code	Tensile strength (MPa)	Predicated tensile strength (MPa)	Elongation at break (%)
PVA/PEG	30.67	30.67	147.34
PVA/PEG/G (0.1%)	24.68	25.62	190.82
PVA/PEG/G (0.2%)	22.12	22.97	209.8
PVA/PEG/G (0.3%)	23.3	20.58	201.6
PVA/PEG/G (0.5%)	23.20	16.31	179.32
PVA/PEG/G (1%)	28.68	8.15	163.24

4. Conclusions

PVA/PEG blends at different PEG loadings were prepared using a solution casting method. A drop in T_g of the PVA/PEG blends was observed as indicated by DSC studies that revealed PEG has a significant plasticization effect on PVA. Such effect was also noticed in FTIR results which showed that the addition of PEG into the blend formed a hydrogen

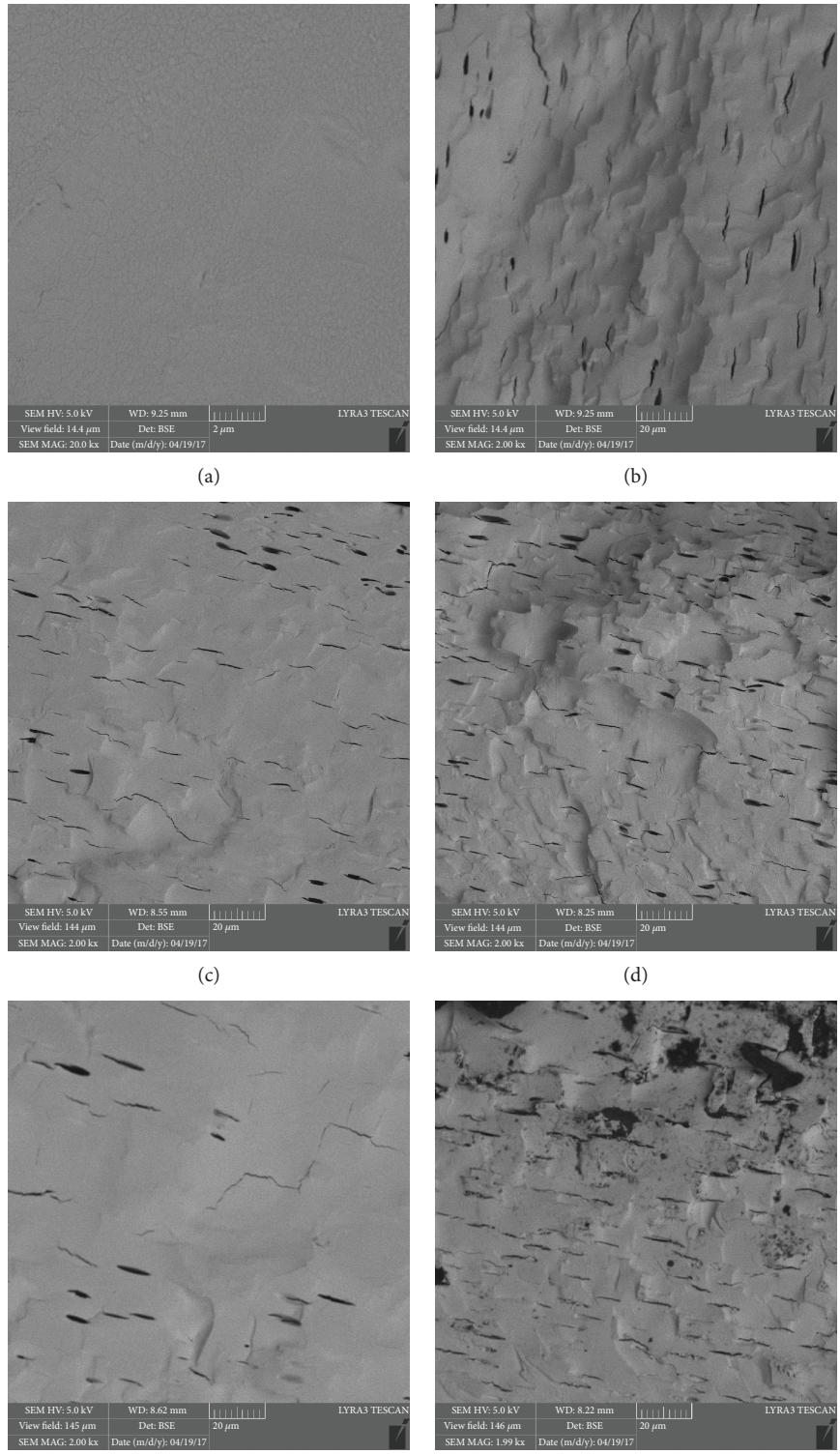

Figure 4: SEM micrographs of PVA/PEG nanocomposites at graphene loadings of (a) 0%, (b) 0.1%, (c) 0.2%, (d) 0.3%, (e) 0.5%, and (f) 1.0%.

bonding between the two polymers. The optimum blend was found at 10 wt% PEG loading, owing to the good compatibility and the improved thermal degradation properties as indicated by SEM and TGA, respectively. The incorporation of 0.2 wt% graphene into the optimum blend increased its elongation at break by 62%. However, not much improvement in the mechanical properties was obtained at higher loading of graphene above 0.3 wt% due to the increase in the brittleness of the obtained nanocomposite films and agglomeration of graphene sheets.

Data Availability

Any additional data can be made available upon request from the corresponding author.

Conflicts of Interest

The authors declare that there is no conflict of interest regarding the publication of this paper.

Acknowledgments

The authors wish to acknowledge the assistance of Deanship of Scientific Research, King Fahd University of Petroleum and Minerals, for their support for providing adequate funds and infrastructure under Project no. FT161010.

References

[1] J. Jose, M. A. Al-Harthi, M. A.-A. AlMa'adeed, J. B. Dakua, and S. K. De, "Effect of graphene loading on thermomechanical properties of poly(vinyl alcohol)/starch blend," *Journal of Applied Polymer Science*, vol. 132, no. 16, 2015.

[2] Z. I. Ali and W. H. Eisa, "Characterization of Electron Beam Irradiated Poly Vinyl Alcohol/Poly Ethylene Glycol Blends," *Journal of Scientific Research*, vol. 6, no. 1, pp. 29–42, 2014.

[3] Y. Li, W. Wu, F. Lin, and A. Xiang, "The interaction between poly(vinyl alcohol) and low-molar-mass poly(ethylene oxide)," *Journal of Applied Polymer Science*, vol. 126, no. 1, pp. 162–168, 2012.

[4] P. A. Sreekumar, M. A. Al-Harthi, and S. K. De, "Effect of glycerol on thermal and mechanical properties of polyvinyl alcohol/starch blends," *Journal of Applied Polymer Science*, vol. 123, no. 1, pp. 135–142, 2012.

[5] P. A. Sreekumar, M. A. Al-Harthi, and S. K. De, "Studies on compatibility of biodegradable starch/polyvinyl alcohol blends," *Polymer Engineering and Science*, vol. 52, no. 10, pp. 2167–2172, 2012.

[6] J. Jose, F. Shehzad, and M. A. Al-Harthi, "Preparation method and physical, mechanical, thermal characterization of poly(vinyl alcohol)/poly(acrylic acid) blends," *Polymer Bulletin*, vol. 71, no. 11, pp. 2787–2802, 2014.

[7] O. A. Bin-Dahman, J. Jose, and M. A. Al-Harithi, "Compatibility of poly(acrylic acid)/starch blends," *Starch - Stärke*, vol. 67, no. 11-12, pp. 1061–1069, 2015.

[8] O. A. Bin-Dahman, J. Jose, and M. A. Al-Harithi, *Starch - Stärke*, vol. 69, no. 7-8, 2017.

[9] J. Jose and M. A. Al-Harthi, "Citric acid crosslinking of poly(-vinyl alcohol)/starch/graphene nanocomposites for superior properties," *Iranian Polymer Journal*, vol. 26, no. 8, pp. 579–587, 2017.

[10] O. Bin-Dahman, M. Rahaman, D. Khastgir, and M. A. Al-Harithi, "Electrical and dielectric properties of poly(vinyl alcohol)/starch/graphene nanocomposites," *The Canadian Journal of Chemical Engineering*, vol. 96, no. 4, pp. 903–911, 2018.

[11] P. A. Sreekumar, M. A. Al-Harthi, and S. K. De, "Reinforcement of starch/polyvinyl alcohol blend using nano-titanium dioxide," *Journal of Composite Materials*, vol. 46, no. 25, pp. 3181–3187, 2012.

[12] S. P. Appu, S. K. De, M. J. Khan, and M. A. Al-Harthi, "Natural weather ageing of starch/polyvinyl alcohol blend: effect of glycerol content," *Journal of Polymer Engineering*, vol. 33, no. 3, pp. 257–263, 2013.

[13] P. A. Sreekumar, M. A. Al-Harthi, M. A. Gondal, and S. K. De, "Heterogeneity of laser-irradiated films of polyvinyl alcohol/starch blends: effect of glycerol content," *Surface and Interface Analysis*, vol. 45, no. 6, pp. 1047–1051, 2013.

[14] J. Jose, S. K. de, M. A. A. AlMa'adeed et al., "Compatibilizing role of carbon nanotubes in poly(vinyl alcohol)/starch blend," *Starch - Stärke*, vol. 67, no. 1-2, pp. 147–153, 2015.

[15] O. A. Bin-Dahman, F. Shehzad, and M. A. al-Harthi, "Influence of graphene on the non-isothermal crystallization kinetics of poly(vinyl alcohol)/starch composite," *Journal of Polymer Research*, vol. 25, no. 1, 2018.

[16] C. K. Chan and I. M. Chu, *Biomaterials*, vol. 23, no. 11, pp. 2353–2358, 2002.

[17] G. Swift, "Water-soluble polymers," *Polymer Degradation and Stability*, vol. 45, no. 2, pp. 215–231, 1994.

[18] R. J. Sengwa, S. Choudhary, and S. Sankhla, "Dielectric properties of montmorillonite clay filled poly(vinyl alcohol)/poly(-ethylene oxide) blend nanocomposites," *Composites Science and Technology*, vol. 70, no. 11, pp. 1621–1627, 2010.

[19] K. Abdel Tawab, M. M. Magida, and S. M. Ibrahim, "Effect of ionizing radiation on the morphological, thermal and mechanical properties of polyvinyl alcohol/polyethylene glycol blends," *Journal of Polymers and the Environment*, vol. 19, no. 2, pp. 440–446, 2011.

[20] R. J. Sengwa and S. Choudhary, "Structural characterization of hydrophilic polymer blends/montmorillonite clay nanocomposites," *Journal of Applied Polymer Science*, vol. 131, no. 16, 2014.

[21] A. M. El Sayed and W. M. Morsi, "Dielectric relaxation and optical properties of polyvinyl chloride/lead monoxide nanocomposites," *Polymer Composites*, vol. 34, no. 12, pp. 2031–2039, 2013.

[22] Z. Guo, D. Zhang, S. Wei et al., "Effects of iron oxide nanoparticles on polyvinyl alcohol: interfacial layer and bulk nanocomposites thin film," *Journal of Nanoparticle Research*, vol. 12, no. 7, pp. 2415–2426, 2010.

[23] X. Yuan, "Enhanced interfacial interaction for effective reinforcement of poly(vinyl alcohol) nanocomposites at low loading of graphene," *Polymer Bulletin*, vol. 67, no. 9, pp. 1785–1797, 2011.

[24] B. W. Chieng, N. A. Ibrahim, W. M. Z. Wan Yunus, and M. Z. Hussein, "Plasticized poly(lactic acid) with low molecular weight poly(ethylene glycol): mechanical, thermal, and morphology properties," *Journal of Applied Polymer Science*, vol. 130, 2013.

[25] A. M. El Sayed and W. M. Morsi, "α-Fe2O3 /(PVA + PEG) nanocomposite films; synthesis, optical, and dielectric characterizations," *Journal of Materials Science*, vol. 49, no. 15, pp. 5378–5387, 2014.

[26] S. G. Abd Alla, H. M. Nizam El-Din, and A. W. M. El-Naggar, "Electron beam synthesis and characterization of poly(vinyl alcohol)/montmorillonite nanocomposites," *Journal of Applied Polymer Science*, vol. 102, no. 2, pp. 1129–1138, 2006.

[27] J. Cheng, J. Zhang, and X. Wang, "Investigation on crystallization behavior and hydrophilicity of poly(vinylidene fluoride)/poly(methyl methacrylate)/poly(vinyl pyrrolidone) ternary

blends by solution casting," *Journal of Applied Polymer Science*, vol. 127, no. 5, pp. 3997–4005, 2013.

[28] Y. Nishio, T. Haratani, T. Takahashi, and R. S. J. Manley, "Cellulose/poly(vinyl alcohol) blends: an estimation of thermodynamic polymer-polymer interaction by melting-point-depression analysis," *Macromolecules*, vol. 22, no. 5, pp. 2547–2549, 1989.

[29] D. M. Bigg, "Mechanical properties of particulate filled polymers," *Polymer Composites*, vol. 8, no. 2, pp. 115–122, 1987.

[30] K. Ghosh and S. N. Maiti, "Mechanical properties of silver-powder-filled polypropylene composites," *Journal of Applied Polymer Science*, vol. 60, no. 3, pp. 323–331, 1996.

[31] L. Nicolais and M. Narkis, "Stress-strain behavior of styrene-acrylonitrile/glass bead composites in the glassy region," *Polymer Engineering and Science*, vol. 11, no. 3, pp. 194–199, 1971.

[32] S. G. Abd Alla, H. M. Said, M. El-Naggar, and A. W. M. El-Naggar, "Structural properties of γ-irradiated poly(vinyl alcohol)/poly(ethylene glycol) polymer blends," *Journal of Applied Polymer Science*, vol. 94, no. 1, pp. 167–176, 2004.

[33] C. S. Reddy, P. K. Babu, K. Sudhakar et al., "Miscibility studies of hydroxyethyl cellulose and poly (ethylene glycol) polymer blends," *Journal of Polymer Research*, vol. 7, pp. 253–266, 2013.

[34] A. K. Mohaparta, S. Mohanty, and S. K. Nayak, "Effect of PEG on PLA/PEG blend and its nanocomposites: a study of thermo-mechanical and morphological characterization," *Polymer Composites*, vol. 35, no. 2, pp. 283–293, 2014.

[35] B. J. Goodfellow and R. H. Wilson, "A fourier transform IR study of the gelation of amylose and amylopectin," *Biopolymers*, vol. 30, no. 13-14, pp. 1183–1189, 1990.

[36] T. Rajavardhana Rao, I. Omkaram, B. Sumalatha, K. Veera Brahmam, and C. Linga Raju, "Electron paramagnetic resonance and optical absorption studies of manganese ions doped in polyvinyl(alcohol) complexed with polyethylene glycol polymer films," *Ionics*, vol. 18, no. 7, pp. 695–701, 2012.

[37] C. Wang, L. Feng, H. Yang et al., "Graphene oxide stabilized polyethylene glycol for heat storage," *Physical Chemistry Chemical Physics*, vol. 14, no. 38, pp. 13233–13238, 2012.

[38] M. Abu Ghalia and Y. Dahman, "Radiation crosslinking polymerization of poly (vinyl alcohol) and poly (ethylene glycol) with controlled drug release," *Journal of Polymer Research*, vol. 22, no. 11, p. 218, 2015.

[39] S. A. Nouh, A. G. Nagla, M. H. Othman, S. A. Eman, and Z. I. Lotfi, *Journal of Applied Polymer Science*, vol. 124, no. 1, pp. 654–660, 2012.

[40] L. Sperling, *Introduction to Physical Polymer Science*, Wiley, New York, 1986, Chapter 4–6.

[41] P. Sakellariou, A. Hassan, and R. C. Rowe, "Interactions and partitioning of diluents/plasticizers in hydroxypropyl methylcellulose and polyvinyl alcohol homopolymers and blends. Part II: Glycerol," *Colloid & Polymer Science*, vol. 272, no. 1, pp. 48–56, 1994.

[42] V. D. Monopoli, L. R. Pizzio, and M. N. Blanco, "Polyvinyl alcohol–polyethylenglycol blends with tungstophosphoric acid addition: Synthesis and characterization," *Materials Chemistry and Physics*, vol. 108, no. 2-3, pp. 331–336, 2008.

[43] Y. Tsuchiya and K. Sumi, "Thermal decomposition products of poly(vinyl alcohol)," *Journal of Polymer Science Part A-1: Polymer Chemistry*, vol. 7, no. 11, pp. 3151–3158, 1969.

[44] A. Ballistreri, S. Foti, G. Montaudo, and E. Scamporrino, "Evolution of aromatic compounds in the thermal decomposition of vinyl polymers," *Journal of Polymer Science: Polymer Chemistry Edition*, vol. 18, no. 4, pp. 1147–1153, 1980.

[45] Y. Yu, Y. Cheng, J. Ren, E. Cao, X. Fu, and W. Guo, "Plasticizing effect of poly(ethylene glycol)s with different molecular weights in poly(lactic acid)/starch blends," *Journal of Applied Polymer Science*, vol. 132, no. 16, 2015.

[46] S. Lee, H. Jin-Yong, and J. Jang, "The effect of graphene nanofiller on the crystallization behavior and mechanical properties of poly(vinyl alcohol)," *Polymer International*, vol. 62, no. 6, pp. 901–908, 2013.

[47] N. C. Bleach, S. N. Nazhat, and K. E. TannerM. Kellomaki and P. T. Tormala, "Effect of filler content on mechanical and dynamic mechanical properties of particulate biphasic calcium phosphate—polylactide composites," *Biomaterials*, vol. 23, no. 7, pp. 1579–1585, 2002.

[48] K. Deshmukh, M. B. Basheer Ahamed, K. K. Sadasivuni et al., "Graphene oxide reinforced polyvinyl alcohol/polyethylene glycol blend composites as high-performance dielectric material," *Journal of Polymer Research*, vol. 23, no. 8, p. 159, 2016.